

# KinectFusion: Real-time 3D Reconstruction and Interaction Using a Moving Depth Camera\*

Shahram Izadi<sup>1</sup>, David Kim<sup>1,3</sup>, Otmar Hilliges<sup>1</sup>, David Molyneaux<sup>1,4</sup>, Richard Newcombe<sup>2</sup>,  
Pushmeet Kohli<sup>1</sup>, Jamie Shotton<sup>1</sup>, Steve Hodges<sup>1</sup>, Dustin Freeman<sup>1,5</sup>,  
Andrew Davison<sup>2</sup>, Andrew Fitzgibbon<sup>1</sup>

<sup>1</sup>Microsoft Research Cambridge, UK      <sup>2</sup>Imperial College London, UK

<sup>3</sup>Newcastle University, UK

<sup>4</sup>Lancaster University, UK

<sup>5</sup>University of Toronto, Canada



Figure 1: KinectFusion enables real-time detailed 3D reconstructions of indoor scenes using only the depth data from a standard Kinect camera. A) user points Kinect at coffee table scene. B) Phong shaded reconstructed 3D model (the wireframe frustum shows current tracked 3D pose of Kinect). C) 3D model texture mapped using Kinect RGB data with real-time particles simulated on the 3D model as reconstruction occurs. D) Multi-touch interactions performed on any reconstructed surface. E) Real-time segmentation and 3D tracking of a physical object.

## ABSTRACT

KinectFusion enables a user holding and moving a standard Kinect camera to rapidly create detailed 3D reconstructions of an indoor scene. Only the depth data from Kinect is used to *track* the 3D pose of the sensor and *reconstruct*, geometrically precise, 3D models of the physical scene in *real-time*. The capabilities of KinectFusion, as well as the novel GPU-based pipeline are described in full. We show uses of the core system for low-cost handheld scanning, and geometry-aware augmented reality and physics-based interactions. Novel extensions to the core GPU pipeline demonstrate object segmentation and user interaction directly in front of the sensor, without degrading camera tracking or reconstruction. These extensions are used to enable real-time multi-touch interactions *anywhere*, allowing any planar or non-planar reconstructed physical surface to be appropriated for touch.

**ACM Classification:** H5.2 [Information Interfaces and Presentation]: User Interfaces. I4.5 [Image Processing and Computer Vision]: Reconstruction. I3.7 [Computer Graphics]: Three-Dimensional Graphics and Realism.

**General terms:** Algorithms, Design, Human Factors.

**Keywords:** 3D, GPU, Surface Reconstruction, Tracking, Depth Cameras, AR, Physics, Geometry-Aware Interactions

\* Research conducted at Microsoft Research Cambridge, UK

Permission to make digital or hard copies of all or part of this work for personal or classroom use is granted without fee provided that copies are not made or distributed for profit or commercial advantage and that copies bear this notice and the full citation on the first page. To copy otherwise, to republish, to post on servers or to redistribute to lists, requires prior specific permission and/or a fee.

UIST'11, October 16-19, 2011, Santa Barbara, CA, USA.

Copyright 2011 ACM 978-1-4503-0716-1/11/10...\$10.00.

## INTRODUCTION

While depth cameras are not conceptually new, Kinect has made such sensors accessible to all. The quality of the depth sensing, given the low-cost and real-time nature of the device, is compelling, and has made the sensor instantly popular with researchers and enthusiasts alike.

The Kinect camera uses a structured light technique [8] to generate real-time *depth maps* containing discrete range measurements of the physical scene. This data can be reprojected as a set of discrete 3D points (or *point cloud*). Even though the Kinect depth data is compelling, particularly compared to other commercially available depth cameras, it is still inherently noisy (see Figures 2B and 3 left). Depth measurements often fluctuate and depth maps contain numerous ‘holes’ where no readings were obtained.

To generate 3D models for use in applications such as gaming, physics, or CAD, higher-level *surface* geometry needs to be inferred from this noisy point-based data. One simple approach makes strong assumptions about the connectivity of neighboring points within the Kinect depth map to generate a *mesh* representation. This, however, leads to noisy and low-quality meshes as shown in Figure 2C. As importantly, this approach creates an incomplete mesh, from only a single, fixed viewpoint. To create a complete (or even watertight) 3D model, different viewpoints of the physical scene must be captured and *fused* into a single representation.

This paper presents a novel interactive reconstruction system called KinectFusion (see Figure 1). The system takes live depth data from a moving Kinect camera and, in real-time, creates a single high-quality, geometrically accurate, 3D model. A user holding a standard Kinect camera can move within any indoor space, and reconstruct a 3D model of the physical scene within seconds. The system contin-



Figure 2: RGB image of scene (A). Extracted normals (B) and surface reconstruction (C) from a single bilateral filtered Kinect depth map. 3D model generated from KinectFusion showing surface normals (D) and rendered with Phong shading (E).

uously tracks the 6 degrees-of-freedom (DOF) pose of the camera and fuses new viewpoints of the scene into a global surface-based representation. A novel GPU pipeline allows for accurate camera tracking and surface reconstruction at interactive real-time rates. This paper details the capabilities of our novel system, as well as the implementation of the GPU pipeline in full.

We demonstrate core uses of KinectFusion as a low-cost handheld scanner, and present novel interactive methods for *segmenting* physical objects of interest from the reconstructed scene. We show how a real-time 3D model can be leveraged for *geometry-aware* augmented reality (AR) and physics-based interactions, where virtual worlds more realistically merge and interact with the real.

Placing such systems into an interaction context, where users need to dynamically interact in front of the sensor, reveals a fundamental challenge – no longer can we assume a static scene for camera tracking or reconstruction. We illustrate failure cases caused by a user moving in front of the sensor. We describe new methods to overcome these limitations, allowing camera tracking and reconstruction of a static background scene, while simultaneously segmenting, reconstructing and tracking foreground objects, including the user. We use this approach to demonstrate real-time multi-touch interactions *anywhere*, allowing a user to appropriate any physical surface, be it planar or non-planar, for touch.

## RELATED WORK

Reconstructing geometry using active sensors [16], passive cameras [11, 18], online images [7], or from unordered 3D points [14, 29] are well-studied areas of research in computer graphics and vision. There is also extensive literature within the AR and robotics community on Simultaneous Localization and Mapping (SLAM), aimed at tracking a user or robot while creating a map of the surrounding physical environment (see [25]). Given this broad topic, and our desire to build a system for *interaction*, this section is structured around specific design goals that differentiate KinectFusion from prior work. The combination of these features makes our interactive reconstruction system unique.

**Interactive rates** Our primary goal with KinectFusion is to achieve real-time interactive rates for *both* camera tracking and 3D reconstruction. This speed is critical for permitting direct feedback and user interaction. This differentiates us from many existing reconstruction systems that support only offline reconstructions [7], real-time but non-interactive rates (e.g. the Kinect-based system of [12] reconstructs at  $\sim 2\text{Hz}$ ),

or support real-time camera tracking but non real-time reconstruction or mapping phases [15, 19, 20].

**No explicit feature detection** Unlike structure from motion (SfM) systems (e.g. [15]) or RGB plus depth (RGBD) techniques (e.g. [12, 13]), which need to robustly and continuously detect sparse scene features, our approach to camera tracking avoids an explicit detection step, and directly works on the full depth maps acquired from the Kinect sensor. Our system also avoids the reliance on RGB (used in recent Kinect RGBD systems e.g. [12]) allowing use in indoor spaces with variable lighting conditions.

**High-quality reconstruction of geometry** A core goal of our work is to capture detailed (or *dense*) 3D models of the real scene. Many SLAM systems (e.g. [15]) focus on real-time tracking, using *sparse* maps for localization rather than reconstruction. Others have used simple point-based representations (such as surfels [12] or aligned point-clouds [13]) for reconstruction. KinectFusion goes beyond these point-based representations by reconstructing *surfaces*, which more accurately approximate real-world geometry.

**Dynamic interaction assumed** We explore tracking and reconstruction in the context of *user interaction*. Given this requirement, it is critical that the representation we use can deal with dynamically changing scenes, where users directly interact in front of the camera. While there has been work on using mesh-based representations for live reconstruction from passive RGB [18, 19, 20] or active Time-of-Flight (ToF) cameras [4, 28], these do not readily deal with changing, dynamic scenes.

**Infrastructure-less** We aim to allow users to explore and reconstruct arbitrary indoor spaces. This suggests a level of mobility, and contrasts with systems that use fixed or large sensors (e.g. [16, 23]) or are fully embedded in the environment (e.g. [26]). We also aim to perform camera tracking without the need for prior augmentation of the space, whether this is the use of infrastructure-heavy tracking systems (e.g. [2]) or fiducial markers (e.g. [27]).

**Room scale** One final requirement is to support whole room reconstructions and interaction. This differentiates KinectFusion from prior dense reconstruction systems, which have either focused on smaller desktop scenes [19, 20] or scanning of small physical objects [4, 28].

The remainder of this paper is structured into two parts: The first provides a high-level description of the capabilities of KinectFusion. The second describes the technical aspects of the system, focusing on our novel GPU pipeline.

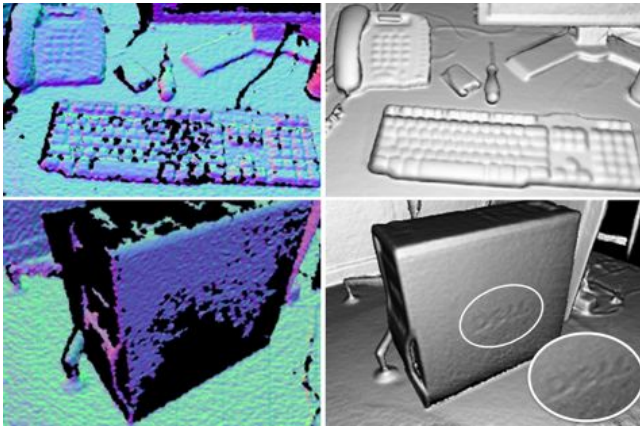


Figure 3: Left: Raw Kinect data (shown as surface normals). Right: Reconstruction shows hole filling and high-quality details such as keys on keyboard, phone number pad, wires, and even a DELL logo on the side of a PC (an engraving less than 1mm deep).

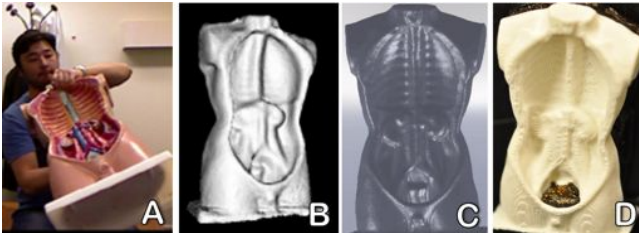


Figure 4: A) User rotating object in front of fixed Kinect. B) 360° 3D reconstruction. C) 3D model imported into SolidWorks. D) 3D printout from reconstruction.

## KINECTFUSION

Our system allows a user to pickup a standard Kinect camera and move rapidly within a room to reconstruct a high-quality, geometrically precise 3D model of the scene. To achieve this, our system continually tracks the 6DOF pose of the camera and fuses live depth data from the camera into a single global 3D model in real-time. As the user explores the space, new views of the physical scene are revealed and these are fused into the same model. The reconstruction therefore grows in detail as new depth measurements are added. Holes are filled, and the model becomes more complete and refined over time (see Figure 3).

Even small motions, caused for example by camera shake, result in new viewpoints of the scene and hence refinements to the model. This creates an effect similar to image super-resolution [6] – adding greater detail than appears visible in the raw signal (see Figure 3). As illustrated in Figures 2 and 3, the reconstructions are high-quality, particularly given the noisy input data and speed of reconstruction. The reconstructed model can also be texture mapped using the Kinect RGB camera (see Figures 1C, 5B and 6A).

**Low-cost Handheld Scanning** A basic and yet compelling use for KinectFusion is as a low-cost object scanner. Although there is a body of research focusing on object scanning using passive and active cameras [4, 28], the speed, quality, and scale of reconstructions have not been demonstrated previously with such low-cost commodity hardware. The mobile and real-time nature of our system allows users to rapidly capture an object from different viewpoints, and

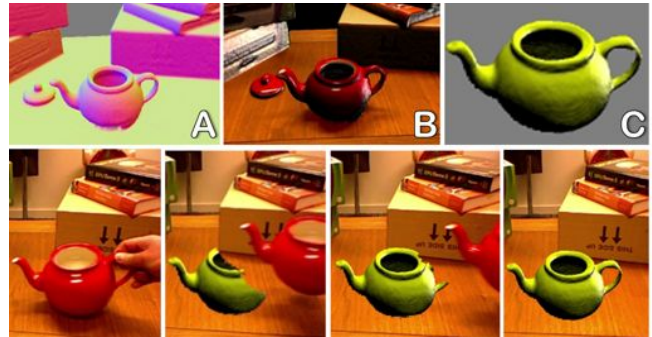


Figure 5: Fast and direct object segmentation. First entire scene is scanned including object of interest – the teapot. 3D reconstruction shows surface normals (A) and texture mapped model (B). Bottom left to right: Teapot physically removed. System monitors real-time changes in reconstruction and colors large changes yellow. C) This achieves accurate segmentation of teapot 3D model from initial scan.

see onscreen feedback immediately. Reconstructed 3D models can be imported into CAD or other 3D modeling applications, or even 3D printed (see Figure 4 C and D).

As also shown in Figure 4, our system can also be used in ‘reverse’ – without any code changes – whereby the system tracks the 6DOF pose of a handheld rigid object that is rotated in front of a fixed Kinect camera (as long as the object occupies the majority of the depth map). While fingers and hands may initially form part of the 3D reconstruction, they are gradually integrated out of the 3D model, because they naturally move as a process of rotating the object.

**Object Segmentation through Direct Interaction** Users may also wish to scan a specific smaller physical object rather than the entire scene. To support this, KinectFusion allows a user to first reconstruct the entire scene, and then accurately *segment* the desired object by moving it physically. The system continuously monitors the 3D reconstruction and observes changes over time. If an object is physically removed from view or moved within the scene by the user, rapid and large changes in the 3D model are observed. Such changes are detected in real-time, allowing the repositioned object to be cleanly segmented from the background model. This approach allows a user to perform segmentation rapidly and without any explicit GUI input, simply by moving the object directly (see Figure 5).

**Geometry-Aware Augmented Reality** Beyond scanning, KinectFusion enables more realistic forms of AR, where a 3D virtual world is overlaid onto and interacts with the real-world representation. Figure 6 (top row) shows a virtual metallic sphere composited directly onto the 3D model, as well as the registered live RGB data from Kinect. The virtual sphere can be rendered from the same perspective as the tracked physical camera, enabling it to be spatially registered as the Kinect moves. As shown in Figure 6 (B, C and D), the live 3D model allows composited virtual graphics to be precisely occluded by the real-world, including geometrically complex objects. This quality of occlusion handling is not possible with the raw depth map (Figure 6E), especially around the edges of objects due to significant noise along depth discontinuities. Precise occlusions are critical for truly immersive AR experiences, and have not been achieved in sparsely mapped real-time AR systems (e.g. [15]).

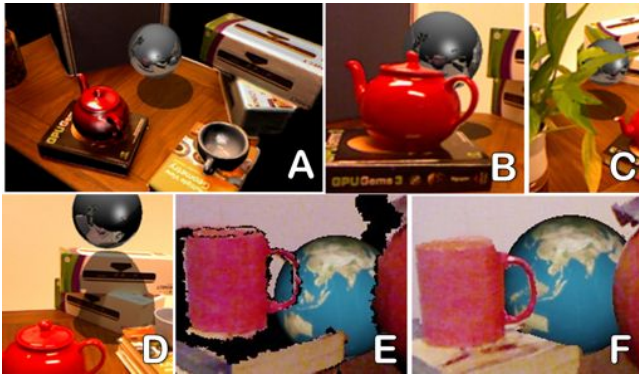


Figure 6: Virtual sphere composited onto texture mapped 3D model (A) and calibrated live Kinect RGB (B, C and D). Real-time 3D model used to handle precise occlusions of the virtual by complex physical geometries (B and C). Comparing occlusion handling using live depth map (E) versus 3D reconstruction (F). Note noise at depth edges, shadows and incomplete data (e.g. book) in live depth map. Virtual sphere casts shadows on physical (D) and reflects parts of the real scene (B and D).



Figure 7: Interactive simulation of physics directly on 3D model even during reconstruction. Thousands of particles interact with reconstructed scene. Reconstruction, camera tracking, and physics simulation all performed in real-time.

Raytraced rendering effects can be calculated in real-time to create realistic shadows, lighting and reflections that consider both virtual and real geometries. For example, Figure 6 (B and D) shows how the virtual can cast shadows onto the real geometry, as well as reflect parts of the real scene onto the virtual. The latter can even be parts of the scene that are occluded from the current perspective of the physical camera.

**Taking Physics Beyond the ‘Surface’** Taking this ability of combining and spatially aligning real and virtual worlds one step further, the virtual can also begin to interact dynamically with the reconstructed scene by simulating aspects of real-world physics. Many types of applications such as gaming and robotics can benefit from such physically precise real-time simulation. Rigid body collisions can be simulated live even as the 3D model is being reconstructed. Figure 7 shows thousands of particles interacting with the 3D model as it is reconstructed, all in real-time. This ability to both re-

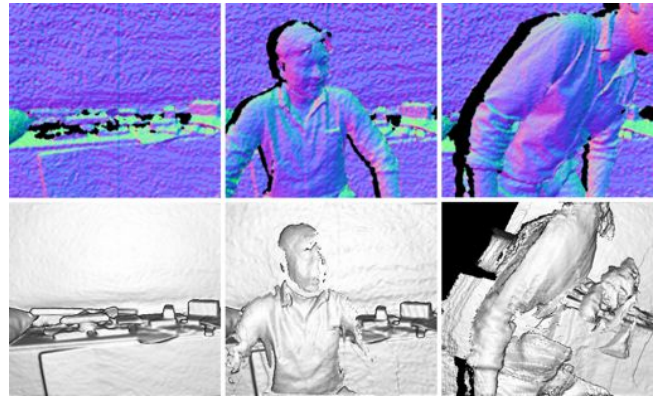


Figure 8: A user moves freely in front of a fixed Kinect. Live raw data (top) and shaded reconstruction (bottom). Left: Scene without user. Middle: User enters scene, but is only partially reconstructed due to motion. Right: Continued scene motions cause tracking failure.

construct a scene and simultaneously perform physics computations on the model is *unique*, and opens up a potential for more physically realistic AR applications.

### Reaching into the Scene

It is important to note that, like most of the related literature on SLAM and camera-based reconstruction, our core system described so far makes a fundamental assumption – that camera tracking will be performed on a *static* scene. Once we switch focus from *reconstructing* the scene towards *interacting* within it, these assumptions no longer hold true. Physical objects such as the user’s hands, will inevitably appear in the scene, move dynamically and impact tracking and reconstruction. Our camera tracking is robust to transient and rapid scene motions (such as the earlier example in Figure 5). However, prolonged interactions with the scene are problematic as illustrated in Figure 8.

While this is clearly a challenging problem within computer vision, our GPU-based pipeline is extended to approximate *camera motion* from *scene motion* for certain user interaction scenarios. When a user is interacting in the scene, the camera tracking ‘locks’ onto the background and ignores the foreground user for camera pose prediction (shown later in Figure 15). This foreground data can be tracked (in 6DOF) and reconstructed independently of camera tracking and reconstruction of the static background.

This ability to reconstruct and track the user in the scene can enable novel extensions to our physics-based simulation shown earlier. Rigid particles can now collide with the rapidly changing dynamic foreground. Figure 9 demonstrates particles interacting with a dynamically updated reconstruction of a moving user. This enables direct interaction between the user and the physics-enabled virtual objects.

Furthermore, as we have captured geometry of both the background scene and foreground user (e.g. hands or potentially the full body), we can determine *intersections* between the two. These points of intersection indicate when the foreground ‘comes into contact with’ the background, and forms a robust method to detect when a user is touching any arbitrarily shaped surface – including non-planar geometries. This allows direct multi-touch interactions, such as those



Figure 9: Interactive simulation of particle physics on dynamic scenes. Particles interact with dynamically moving foreground user, whilst physical camera and user move. User can collide with the physics-enabled virtual objects.

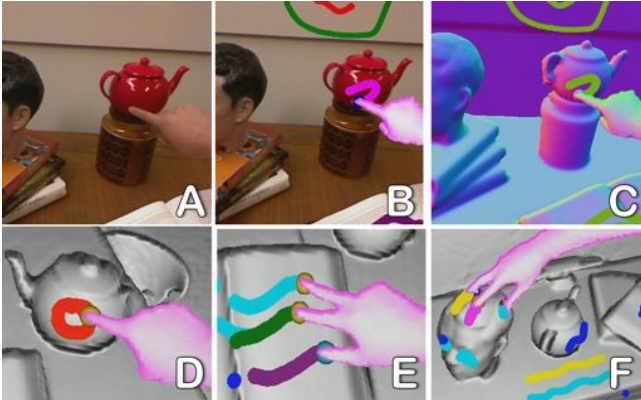


Figure 10: Enabling touch input on arbitrary surfaces with a moving camera. A) Live RGB. B) Compositing view with segmented hand and single finger touching curved surface. C) rendered as surface normals. D) Single finger drawing on a curved surface. E) Multi-touch on regular planar book surface. F) Multi-touch on an arbitrarily shaped surface.

demonstrated in the interactive tabletop community, to reach any surface in the user’s environment (see Figure 10).

### GPU IMPLEMENTATION

Our approach for real-time camera tracking and surface reconstruction is based on two well-studied algorithms [1, 5, 24], which have been designed from the ground-up for parallel execution on the GPU. A full formulation of our method is provided in [21], as well as quantitative evaluation of reconstruction performance. The focus of this section is on the implementation of our novel core and extended GPU pipeline, which is critical in enabling interactive rates.

The main system pipeline consists of four main stages (labeled appropriately in Figure 11):

- a) Depth Map Conversion** The live depth map is converted from image coordinates into 3D points (referred to as vertices) and normals in the coordinate space of the camera.
- b) Camera Tracking** In the tracking phase, a rigid 6DOF transform is computed to closely align the current oriented points with the previous frame, using a GPU implementation of the Iterative Closest Point (ICP) algorithm [1]. Relative transforms are incrementally applied to a single transform that defines the global pose of the Kinect.
- c) Volumetric Integration** Instead of fusing point clouds or creating a mesh, we use a volumetric surface representation based on [5]. Given the global pose of the camera, oriented points are converted into global coordinates, and a single 3D voxel grid is updated. Each voxel stores a running average of its distance to the assumed position of a physical surface.
- d) Raycasting** Finally, the volume is raycast to extract views of the implicit surface, for rendering to the user. When using the global pose of the camera, this raycasted view of the

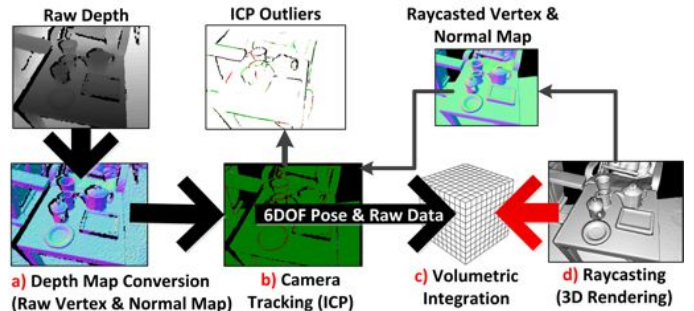


Figure 11: Overview of tracking and reconstruction pipeline from raw depth map to rendered view of 3D scene.

volume also equates to a synthetic depth map, which can be used as a less noisy more globally consistent reference frame for the next iteration of ICP. This allows tracking by aligning the current live depth map with our less noisy raycasted view of the model, as opposed to using only the live depth maps frame-to-frame.

Each of these steps is executed in parallel on the GPU using the CUDA language. We describe each of these steps of the pipeline in the following sections.

### Depth Map Conversion

At time  $i$ , each CUDA thread operates in parallel on a separate pixel  $\mathbf{u} = (x, y)$  in the incoming depth map  $\mathbf{D}_i(\mathbf{u})$ . Given the intrinsic calibration matrix  $\mathbf{K}$  (of the Kinect infrared camera), each GPU thread reprojects a specific depth measurement as a 3D vertex in the camera’s coordinate space as follows:  $\mathbf{v}_i(\mathbf{u}) = \mathbf{D}_i(\mathbf{u}) \mathbf{K}^{-1}[\mathbf{u}, 1]$ . This results in a single vertex map  $\mathbf{V}_i$  computed in parallel.

Corresponding normal vectors for each vertex are computed by each GPU thread using neighboring reprojected points:  $\mathbf{n}_i(\mathbf{u}) = (\mathbf{v}_i(x+1, y) - \mathbf{v}_i(x, y)) \times (\mathbf{v}_i(x, y+1) - \mathbf{v}_i(x, y))$  (normalized to unit length  $\mathbf{n}_i/||\mathbf{n}_i||$ ). This results in a single normal map  $\mathbf{N}_i$  computed in parallel.

The 6DOF camera pose at time  $i$  is a rigid body transform matrix  $\mathbf{T}_i = [\mathbf{R}_i | \mathbf{t}_i]$  containing a 3x3 rotation matrix ( $\mathbf{R}_i$ ) and 3D translation vector ( $\mathbf{t}_i$ ). Given this transform, a vertex and normal can be converted into global coordinates:  $\mathbf{v}_i^g(\mathbf{u}) = \mathbf{T}_i \mathbf{v}_i(\mathbf{u})$  and  $\mathbf{n}_i^g(\mathbf{u}) = \mathbf{R}_i \mathbf{n}_i(\mathbf{u})$  respectively.

### Camera Tracking

ICP is a popular and well-studied algorithm for 3D shape alignment (see [24] for a detailed study). In KinectFusion, ICP is instead leveraged to track the camera pose for each new depth frame, by estimating a single 6DOF transform that closely aligns the current oriented points with those of the previous frame. This gives a relative 6DOF transform which can be incrementally applied together to give the single global camera pose  $\mathbf{T}_i$ .

The important first step of ICP is to find correspondences between the current oriented points at time  $i$  with the previous at  $i-1$ . In our system we use *projective data association* [24] to find these correspondences. This part of the GPU-based algorithm is shown as pseudocode in Listing 1. Given the previous global camera pose  $\mathbf{T}_{i-1}$ , each GPU thread transforms a unique point  $\mathbf{v}_{i-1}$  into camera coordinate space, and perspective projects it into image coordinates. It then uses this 2D point as a lookup into the current vertex ( $\mathbf{V}_i$ ) and normal

maps ( $\mathbf{N}_i$ ), finding corresponding points along the *ray* (i.e. projected onto the same image coordinates). Finally, each GPU thread tests the compatibility of corresponding points to reject *outliers*, by first converting both into global coordinates, and then testing that the Euclidean distance and angle between them are within a threshold. Note that  $\mathbf{T}_i$  is initialized with  $\mathbf{T}_{i-1}$  and is updated with an incremental transform calculated per iteration of ICP.

---

**Listing 1** Projective point-plane data association.

---

```

1: for each image pixel  $\mathbf{u} \in$  depth map  $\mathbf{D}_i$  in parallel do
2:   if  $\mathbf{D}_i(\mathbf{u}) > 0$  then
3:      $\mathbf{v}_{i-1} \leftarrow \mathbf{T}_{i-1}^{-1} \mathbf{v}_{i-1}^g$ 
4:      $\mathbf{p} \leftarrow$  perspective project vertex  $\mathbf{v}_{i-1}$ 
5:     if  $\mathbf{p} \in$  vertex map  $\mathbf{V}_i$  then
6:        $\mathbf{v} \leftarrow \mathbf{T}_i \mathbf{V}_i(\mathbf{p})$ 
7:        $\mathbf{n} \leftarrow \mathbf{R}_i \mathbf{N}_i(\mathbf{p})$ 
8:       if  $\|\mathbf{v} - \mathbf{v}_{i-1}^g\| <$  distance threshold and
          $abs(\mathbf{n} \cdot \mathbf{n}_{i-1}^g) <$  normal threshold then
9:         point correspondence found

```

---

Given these set of corresponding oriented points, the output of each ICP iteration is a single transformation matrix  $\mathbf{T}$  that minimizes the point-to-plane error metric [3], defined as the sum of squared distances between each point in the current frame and the tangent plane at its corresponding point in the previous frame:

$$\arg \min_{\mathbf{u}} \sum_{\mathbf{D}_i(\mathbf{u}) > 0} \|(\mathbf{T}\mathbf{v}_i(\mathbf{u}) - \mathbf{v}_{i-1}^g(\mathbf{u})) \cdot \mathbf{n}_{i-1}^g(\mathbf{u})\|^2 \quad (1)$$

We make a linear approximation to solve this system, by assuming only an incremental transformation occurs between frames [3, 17]. The linear system is computed and summed in parallel on the GPU using a tree reduction. The solution to this 6x6 linear system is then solved on the CPU using a Cholesky decomposition.

One of the key novel contributions of our GPU-based camera tracking implementation is that ICP is performed on *all* the measurements provided in each  $640 \times 480$  Kinect depth map. There is no sparse sampling of points or need to explicitly extract features (although of course ICP does implicitly require depth features to converge). This type of *dense* tracking is only feasible due to our novel GPU implementation, and plays a central role in enabling segmentation and user interaction in KinectFusion, as described later.

### Volumetric Representation

By predicting the global pose of the camera using ICP, any depth measurement can be converted from image coordinates into a single consistent global coordinate space. We integrate this data using a *volumetric* representation based on [5]. A 3D volume of fixed resolution is predefined, which maps to specific dimensions of a 3D physical space. This volume is subdivided uniformly into a 3D grid of voxels. Global 3D vertices are integrated into voxels using a variant of Signed Distance Functions (SDFs) [22], specifying a relative distance to the actual surface. These values are positive in-front of the surface, negative behind, with the surface interface defined by the *zero-crossing* where the values change sign.

In practice, we only store a truncated region around the actual surface [5] – referred to in this paper as Truncated Signed

Distance Functions (TSDFs). We have found this representation has many advantages for the Kinect sensor data, particularly when compared to other representations such as meshes. It implicitly encodes uncertainty in the range data, efficiently deals with multiple measurements, fills holes as new measurements are added, accommodates sensor motion, and implicitly stores surface geometry.

---

**Listing 2** Projective TSDF integration leveraging coalesced memory access.

---

```

1: for each voxel  $\mathbf{g}$  in x,y volume slice in parallel do
2:   while sweeping from front slice to back do
3:      $\mathbf{v}^g \leftarrow$  convert  $\mathbf{g}$  from grid to global 3D position
4:      $\mathbf{v} \leftarrow \mathbf{T}_i^{-1} \mathbf{v}^g$ 
5:      $\mathbf{p} \leftarrow$  perspective project vertex  $\mathbf{v}$ 
6:     if  $\mathbf{v}$  in camera view frustum then
7:        $sdf_i \leftarrow \|\mathbf{t}_i - \mathbf{v}^g\| - \mathbf{D}_i(\mathbf{p})$ 
8:       if ( $sdf_i > 0$ ) then
9:          $tsdf_i \leftarrow min(1, sdf_i / \text{max truncation})$ 
10:      else
11:         $tsdf_i \leftarrow max(-1, sdf_i / \text{min truncation})$ 
12:       $\mathbf{w}_i \leftarrow min(\text{max weight}, \mathbf{w}_{i-1} + 1)$ 
13:       $tsdf^{avg} \leftarrow \frac{tsdf_{i-1} \mathbf{w}_{i-1} + tsdf_i \mathbf{w}_i}{\mathbf{w}_{i-1} + \mathbf{w}_i}$ 
14:      store  $\mathbf{w}_i$  and  $tsdf^{avg}$  at voxel  $\mathbf{g}$ 

```

---

**Volumetric Integration** To achieve real-time rates, we describe a novel GPU implementation of volumetric TSDFs. The full 3D voxel grid is allocated on the GPU as aligned linear memory. Whilst clearly not memory efficient (a  $512^3$  volume containing 32-bit voxels requires 512MB of memory), our approach is *speed* efficient. Given the memory is aligned, access from parallel threads can be *coalesced* to increase memory throughput.

The algorithm ensures coalesced access to the voxel grid, whilst integrating depth data *projectively*. The algorithm updates TSDF values in the volume at real-time rates (as quickly as 2ms for a  $512^3$  volume), and allows continuous surface estimates to be discretized into the voxel grid, from the point-based Kinect depth maps. Furthermore, this approach is *much* simpler to implement than hierarchical techniques (e.g. [29]), but with the increased available memory on commodity GPUs, can scale to modeling a whole room.

The pseudocode Listing 2 illustrates the main steps of our algorithm. Due to the large number of voxels typically within a volume, it is not feasible to launch a GPU thread per voxel. To ensure coalesced memory access, a GPU thread is assigned to each (x, y) position on the front slice of the volume. In parallel, GPU threads then sweep through the volume, moving along each slice on the Z-axis. Given the resolution of the volume, and the physical dimensions this maps to, each discrete 3D grid location can be converted into a vertex in global coordinates. A metric distance from the camera center (the translation vector of the global camera transform) to this vertex can be calculated. This 3D vertex can also be perspective projected back into image coordinates to lookup the actual depth measurement along the ray. The difference between measured and calculated distances gives a new SDF value for the voxel (line 7). This is normalized to a TSDF (lines 9 and 11) and averaged with the previous stored value

using a simple running weighted average (line 13) [5]. Both the new weight and averaged TSDF are stored at the voxel.

**Raycasting for Rendering and Tracking** A GPU-based raycaster is implemented to generate views of the implicit surface within the volume for rendering and tracking (see pseudocode Listing 3). In parallel, each GPU thread walks a single ray and renders a single pixel in the output image. Given a starting position and direction of the ray, each GPU thread traverses voxels along the ray, and extracts the position of the implicit surface by observing a zero-crossing (a change in the sign of TSDF values stored along the ray). The final surface intersection point is computed using a simple linear interpolation given the trilinearly sampled points either side of the zero-crossing. Assuming the gradient is orthogonal to the surface interface, the surface normal is computed directly as the derivative of the TSDF at the zero-crossing [22]. Therefore each GPU thread that finds a ray/surface intersection can calculate a single interpolated vertex and normal, which can be used as parameters for lighting calculations on the output pixel, in order to render the surface.

**Listing 3** Raycasting to extract the implicit surface, composite virtual 3D graphics, and perform lighting operations.

```

1: for each pixel  $\mathbf{u}$  in output image in parallel do
2:    $\mathbf{ray}^{\text{start}} \leftarrow$  back project [ $\mathbf{u}$ , 0]; convert to grid pos
3:    $\mathbf{ray}^{\text{next}} \leftarrow$  back project [ $\mathbf{u}$ , 1]; convert to grid pos
4:    $\mathbf{ray}^{\text{dir}} \leftarrow$  normalize ( $\mathbf{ray}^{\text{next}} - \mathbf{ray}^{\text{start}}$ )
5:    $\mathbf{ray}^{\text{len}} \leftarrow 0$ 
6:    $\mathbf{g} \leftarrow$  first voxel along  $\mathbf{ray}^{\text{dir}}$ 
7:    $\mathbf{m} \leftarrow$  convert global mesh vertex to grid pos
8:    $\mathbf{m}^{\text{dist}} \leftarrow \|\mathbf{ray}^{\text{start}} - \mathbf{m}\|$ 
9:   while voxel  $\mathbf{g}$  within volume bounds do
10:     $\mathbf{ray}^{\text{len}} \leftarrow \mathbf{ray}^{\text{len}} + 1$ 
11:     $\mathbf{g}^{\text{prev}} \leftarrow \mathbf{g}$ 
12:     $\mathbf{g} \leftarrow$  traverse next voxel along  $\mathbf{ray}^{\text{dir}}$ 
13:    if zero crossing from  $\mathbf{g}$  to  $\mathbf{g}^{\text{prev}}$  then
14:       $\mathbf{p} \leftarrow$  extract trilinear interpolated grid position
15:       $\mathbf{v} \leftarrow$  convert  $\mathbf{p}$  from grid to global 3D position
16:       $\mathbf{n} \leftarrow$  extract surface gradient as  $\nabla \text{tsdf}(\mathbf{p})$ 
17:      shade pixel for oriented point ( $\mathbf{v}$ ,  $\mathbf{n}$ ) or
18:      follow secondary ray (shadows, reflections, etc)
19:    if  $\mathbf{ray}^{\text{len}} > \mathbf{m}^{\text{dist}}$  then
20:      shade pixel using inputted mesh maps or
21:      follow secondary ray (shadows, reflections, etc)

```

Our rendering pipeline shown in Figure 12 also allows conventional polygon-based graphics to be *composited* on the raycasted view, enabling blending of virtual and real scenes with correct occlusion handling (see Figure 6). In the first step (labeled a), a mesh-based scene is rendered with *graphics camera* parameters identical to the physical global camera pose ( $\mathbf{T}_i$ ) and intrinsics ( $\mathbf{K}$ ). Instead of rendering to the framebuffer, the vertex buffer, surface normals and unshaded color data are stored in off-screen vertex, normal and color maps respectively (labeled b), and used as input during raycasting (labeled c). For each GPU thread, a distance from the associated mesh vertex to the camera center is calculated in grid coordinates (Listing 3 lines 7 and 8). This distance acts as an additional termination condition while stepping along each ray (line 19), allowing accurate occlusion testing between volumetric and mesh surface geometries.

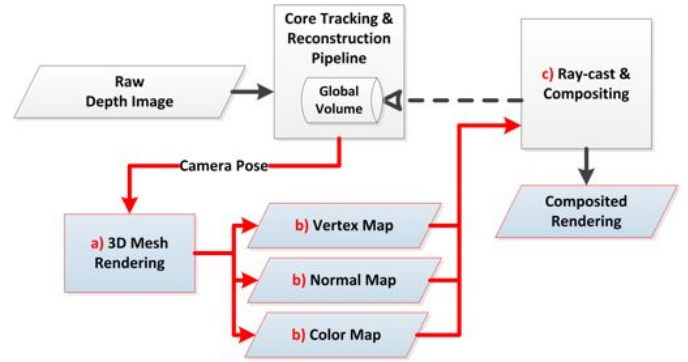


Figure 12: Rendering pipeline combining raycasting of volume with compositing of virtual polygon-based graphics.

Ambient, diffuse and specular lighting contributions can be calculated *across* reconstructed and virtual geometries (see Figure 6). More advanced shading calculations can be performed by walking along the second (and possibly further) bounce of each ray. Shadows are calculated after the first ray hits a voxel or mesh surface (Listing 3 line 13 and 19), by walking a secondary ray from the surface to light position (using grid coordinates). If a surface is hit before ray termination then the vertex is shadowed. For reflections, once the first ray hits a surface, a new ray direction is calculated, based on the surface normal and initial ray direction.

A novel contribution of our raycaster is the ability to view the implicit surface of the reconstructed 3D model, composite polygon geometry with correct occlusion handling, and provide advanced shading requiring raytraced operations, all in real-time, through a single algorithm. Any 6DOF graphics camera transform can be used to raycast the volume, including arbitrary third-person views allowing user navigation of the 3D model. However, another *key* contribution of our raycaster, is in generating higher-quality data for ICP camera tracking. When the raycast camera transform equates to the physical camera pose, the extracted vertices and normals equate to depth and normal maps (from the same perspective as the physical camera) but with considerably less noise, shadows and holes than the raw Kinect data. As shown in [21], this allows us to mitigate issues of drift and reduce ICP errors, by tracking directly from the raycasted model as opposed to frame-to-frame ICP tracking.

### Simulating Real-World Physics

Taking the merging of real and virtual geometries further, the GPU pipeline is extended to support simulation of physically realistic collisions between virtual objects and the reconstructed scene. A particle simulation is implemented on the GPU, based on [9] and [10]. Scene geometry is represented within the simulation by a set of static particles (see Figure 13). These are spheres of identical size, which remain stationary but can collide with other dynamically simulated particles. Whilst an approximation, this technique models every discrete surface voxel within the volume in real-time, achieving compelling results even for very small and arbitrarily shaped objects such as a book’s edges or a teapot’s handle in Figures 7 (bottom right) and 13.

Static particles are created during volume integration. As the volume is swept, TSDF values within an adaptive threshold close to zero (defining the surface interface or *zero level*

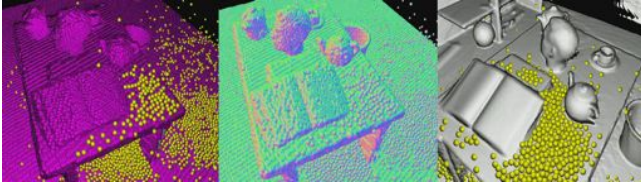


Figure 13: Simulating physics on the real-time reconstruction. Left: Surface is approximated as series of static particles (updated per integration sweep) which interact with dynamic particles. Every surface voxel is represented by a static particle. Middle: Surface normals of static and dynamic particles. Right: Shaded scene with only dynamic particles composited.

*set*) are extracted. For each surface voxel, a static particle is instantiated. Each particle contains a 3D vertex in global (metric) space, a velocity vector (always empty for static particles), and an ID. One key challenge then becomes detecting collisions. We use a spatially subdivided uniform grid to identify neighboring particles [9]. Each cell in the grid has a unique ID. Each dynamic or static particle is assigned a grid cell ID by converting the particle’s global vertex to grid coordinates. Our system then maintains two lists – one containing static particles; the other dynamic. In both, particles are binned into the grid cells by sorting them by their current grid ID (using a GPU-based radix sort). During each simulation step, a GPU thread is launched per dynamic particle. Each thread processes collisions by examining ( $3^3$ ) neighborhood of cells (first for dynamic-dynamic collisions and then dynamic-static). The Discrete Element Method (DEM) [10] is used to calculate a velocity vector when two particles collide. The particle’s global velocity is incremented based on all neighboring collisions, gravity, and interactions with the bounding volume. Each particle is then repositioned based on the accumulated velocity per simulation step.

Figure 7 shows thousands of particles interacting with the reconstructed scene. A major contribution of our GPU-based pipeline is that it maintains interactive rates despite the overhead of physics simulation, whilst performing real-time camera tracking and reconstruction. By default, only dynamic particles are rendered during raycasting and again can be correctly occluded by the reconstructed geometry (see Figure 7).

### INTERACTING IN THE SCENE

The core system described so far makes assumptions that the scene will remain reasonably static. Clearly in an interaction context, users want to move freely in front of the sensor, and interact in the scene. This opens up two main challenges.

First, ICP tracking assumes a single rigid transform occurred per frame due to camera motion. User interaction in front of the sensor will cause scene motion *independent* of camera motion, which breaks this assumption. Because our ICP tracking is dense (i.e. uses all available points) our system is resilient to transient scene motions. For example, in Figure 5, even when the user moves the object, enough *background* points will remain for ICP to converge. However, large or longer-term scene motions will cause tracking failure.

Second, whilst our system supports real-time reconstruction, surface predictions are refined over time using a running weighted average of distance values. By adapting the weighting, higher precedence can be given to new TSDF values, allowing for faster model updates, but the trade-off is addi-

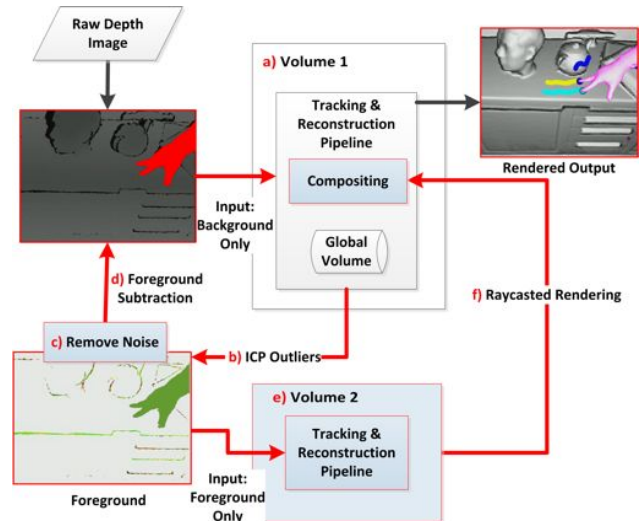


Figure 14: Extended GPU pipeline for real-time foreground and background segmentation, tracking and reconstruction.

tional noise being introduced to the reconstruction. In practice, a weight is chosen to balance quality of reconstruction with regular updates to the reconstruction based on scene changes. However, this does not support a continuously moving scene. Typically a user freely moving in the scene leads to associated depth data being partially integrated into the volume (Figure 8 middle). As camera tracking relies directly on this model, which is now inconsistent with the live data, failures will occur (Figure 8 right).

**ICP Outliers for Segmentation** To begin to explore dynamic user interaction with the reconstructed scene, a novel extension to the core GPU pipeline is provided (shown in Figure 14). The technique leverages a unique property of dense ICP tracking. When *all* depth measurements are used, *outliers* from projective data association can form a strong initial prediction as to parts of the scene moving independent of camera motion – if enough rigid background points are present for ICP still to converge. Our solution robustly *segments* a moving foreground object from the background, allowing tracking failures to be reduced, and enabling users to interact directly in the scene.

This pipeline assumes that at least parts of a rigid scene have been initially reconstructed using the core reconstruction pipeline (labeled a). After this initial scan, a moving object entering the scene contains oriented points with significant disparity to already reconstructed surfaces. These fail ICP projective data association and are copied into an *outlier map* (labeled b). Next, a depth-aware connected component analysis is performed on the outlier map to cluster large connected patches and remove smaller outliers due to sensor noise (labeled c). Large connected patches, where foreground scene motion has been detected, are masked in the input depth map for core ‘background’ reconstruction (labeled d). This stops associated foreground depth measurements being used for reconstruction or tracking in the core pipeline. Large patches of outliers can be additionally reconstructed using a second volume (labeled e) – potentially running on a separate GPU with different reconstruction settings. A final step raycasts the two separate volumes and composites the output (labeled f), using the same method as Figure 12.





Figure 15: Moving user is segmented and reconstructed, independent of background. Left to right: 1) Live RGB. 2) ICP outliers (for initial segmentation prediction). 3) final composited scene showing foreground shaded differently to background. 4) Composited normal maps.

Overall our technique yields compelling results in stabilizing tracking and therefore improving reconstruction quality for a static background, even when parts of the scene continually move in front of the camera. Furthermore, it allows a foreground object to be robustly segmented, and potentially reconstructed separately of the background (see Figure 15).

**Listing 4** Create touch map – testing if foreground and background vertices overlap.

```

1:  $\mathbf{V}_{fg}^g \leftarrow$  raycasted vertex map from foreground volume
2: for each pixel  $\mathbf{u} \in \mathbf{O}$  (touch map) in parallel do
3:   cast single ray for  $\mathbf{u}$  (as Listing 3)
4:   if zero crossing when walking ray then
5:      $\mathbf{v}_{bg}^g \leftarrow$  interpolated global zero crossing position
6:     if  $\|\mathbf{v}_{bg}^g - \mathbf{V}_{fg}^g(\mathbf{u})\| <$  adaptive threshold then
7:        $\mathbf{O}(\mathbf{u}) \leftarrow \mathbf{V}_{fg}^g(\mathbf{u})$ 

```

**Detecting Touch on Arbitrary Surfaces** The pipeline can be further extended to support multi-touch input by observing intersections between foreground and background. We extend the default raycasting of the background volume to output a touch map, as shown in pseudocode Listing 4. Using the raycasted foreground vertex map as input, each GPU thread again walks a ray through the background volume. If a zero crossing is located, the corresponding foreground vertex (along the same ray) is tested (line 6). If foreground and background are within range, the foreground position is output in the touch map. A depth-aware connected component analysis of the touch map suppresses noise and labels fingertip candidates, which are tracked over time. Examples of enabling multi-touch on both planar and non-planar surfaces are shown in Figures 10 and 16.

### Towards Modeling of Dynamic Scenes

The ability of now distinguishing moving foreground robustly from background raises interesting questions regarding how best to reconstruct such moving surfaces. The key challenge becomes how to integrate foreground data into a second volume so that correspondence between surface measurements can be ensured over time. As an initial exploration, we have experimented with independently predicting the pose of the foreground object using another instance of



Figure 16: Segmentation, tracking and reconstruction of user's arm with moving Kinect. Top left: Arm is first introduced and reconstruction contains a great deal of noise. Top right: surface is refined based on separate ICP-based pose prediction. Bottom left: the moving surface is rapidly reconstructed to a much higher quality than the raw Kinect signal. Bottom right: The intersection between foreground and background surfaces are used for multi-touch detection.

ICP. Again *dense* ICP is performed but only using the *foreground* oriented points (from the live depth map and ray-casted second volume). In practice we have found that dense ICP converges even if small parts of the foreground are moving non-rigidly. A compelling example is a user's arm (Figure 15) where ICP converges on the rigid parts even if fingers are moving non-rigidly. This offers a coarse method for predicting the pose of the foreground object, relative to the global camera transform.

Using this predicted pose, depth measurements can be aligned and fused into the second volume. A surface prediction of the foreground, which becomes more refined and complete, can be built up over time. Because the foreground surface will likely be moving, we give more weight to new measurements being integrated. One simple extension uses a per-voxel weighting, adapted based on a running average of the derivative of the TSDF (prior to integration). This allows us to adapt the weight of individual surface voxels, giving higher priority to new measurements when the rate of change is high (e.g. fingers or hands), and lower if the TSDF measurements are stable (e.g. the forearm). Figures 16 and 15 shows our initial results based on foreground ICP tracking and per-voxel adaptive weighting. Note there is considerably less noise than the raw Kinect data – the user's arms, hand and fingers are clearly identifiable – and that this foreground reconstruction occurs alongside camera tracking and refinement of the background reconstruction.

For our physics simulation, we can now represent the entire foreground reconstruction as static particles, allowing collisions between the moving user, and the dynamic particles, to be modeled per frame (as shown in Figure 9). This approach of reconstructing a moving foreground, can also be used purely to *track* the pose of rigid objects held in the user's hand – enabling tracking independent of camera motion and without markers or prior knowledge of the object. One example is shown in Figure 1 (far right) where an already reconstructed teapot (from Figure 5) is tracked in 6DOF and re-registered with the real physical object.

### CONCLUSIONS

We have presented KinectFusion, a real-time 3D reconstruction and interaction system using a moving standard Kinect. Our contributions are threefold. First, we detailed a novel

GPU pipeline that achieves 3D tracking, reconstruction, segmentation, rendering, and interaction, all in real-time using only a commodity camera and graphics hardware. Second, we have demonstrated core novel uses for our system: for low-cost object scanning and advanced AR and physics-based interactions. Third, we described new methods for segmenting, tracking and reconstructing dynamic users and the background scene simultaneously, enabling multi-touch on any indoor scene with arbitrary surface geometries. We believe this is the first time that a reconstruction system has shown this level of user interaction directly in the scene.

Our hope is to scale the system further, reconstructing larger scenes where more memory efficient representations such as octrees might be needed [29]. Encouraged by our initial results, we also wish to explore more fine-grained methods for tracking and reconstruction of moving deformable surfaces, including the user. Our hope is that KinectFusion will open many new topics for research both in terms of the underlying technology, as well as the interactive possibilities it enables.

## REFERENCES

1. P. J. Besl and N. D. McKay. A method for registration of 3D shapes. *IEEE Trans. Pattern Anal. Mach. Intell.*, 14:239–256, February 1992.
2. X. Cao and R. Balakrishnan. Interacting with dynamically defined information spaces using a handheld projector and a pen. In *UIST*, pages 225–234, 2006.
3. Y. Chen and G. Medioni. Object modeling by registration of multiple range images. *Image and Vision Computing (IVC)*, 10(3):145–155, 1992.
4. Y. Cui et al. 3D shape scanning with a time-of-flight camera. In *Computer Vision and Pattern Recognition (CVPR)*, pages 1173–1180, June 2010.
5. B. Curless and M. Levoy. A volumetric method for building complex models from range images. *ACM Trans. Graph.*, 1996.
6. S. Farsiu et al. Fast and robust multiframe super resolution. *IEEE Transactions on Image Processing*, 13(10):1327–1344, 2004.
7. J. Frahm et al. Building Rome on a cloudless day. In *Proc. Europ. Conf. on Computer Vision (ECCV)*, 2010.
8. B. Freedman, A. Shpunt, M. Machline, and Y. Arieli. Depth mapping using projected patterns. Patent Application, 10 2008. WO 2008/120217 A2.
9. S. L. Grand. Broad-phase collision detection with CUDA. In *GPU Gems 3*. Addison-Wesley, 2007.
10. T. Harada. Real-time rigid body simulation on GPUs. In *GPU Gems 3*. Addison-Wesley Professional, 2007.
11. R. Hartley and A. Zisserman. *Multiple view geometry in computer vision*. Cambridge University Press, second edition, 2004.
12. P. Henry et al. RGB-D mapping: Using depth cameras for dense 3D modeling of indoor environments. In *Proc. of the Int. Symposium on Experimental Robotics (ISER)*, 2010.
13. B. Huhle et al. Fusion of range and color images for denoising and resolution enhancement with a non-local filter. *Computer Vision and Image Understanding*, 114(12):1336–1345, 2010.
14. M. Kazhdan, M. Bolitho, and H. Hoppe. Poisson surface reconstruction. In *Proc. of the Eurographics Symposium on Geometry Processing*, 2006.
15. G. Klein and D. W. Murray. Parallel tracking and mapping for small AR workspaces. In *ISMAR*, 2007.
16. M. Levoy et al. The digital Michelangelo project: 3D scanning of large statues. *ACM Trans. Graph.*, 2000.
17. K. Low. Linear least-squares optimization for point-to-plane ICP surface registration. Technical report, TR04-004, University of North Carolina, 2004.
18. P. Merrell et al. Real-time visibility-based fusion of depth maps. In *Proc. of the Int. Conf. on Computer Vision (ICCV)*, 2007.
19. R. A. Newcombe and A. J. Davison. Live dense reconstruction with a single moving camera. In *Proc. of the IEEE CVPR*, 2010.
20. R. A. Newcombe, S. Lovegrove, and A. J. Davison. DTAM: Dense tracking and mapping in real-time. In *Proc. of the Int. Conf. on Computer Vision (ICCV)*, 2011.
21. R. A. Newcombe et al. KinectFusion: Real-time dense surface mapping and tracking. In *ISMAR*, 2011.
22. S. Osher and R. Fedkiw. *Level set methods and dynamic implicit surfaces*. Springer, 2002.
23. S. Rusinkiewicz, O. Hall-Holt, and M. Levoy. Real-time 3D model acquisition. *ACM Trans. Graph.*, 2002.
24. S. Rusinkiewicz and M. Levoy. Efficient variants of the ICP algorithm. *3D Digital Imaging and Modeling, Int. Conf. on*, 0:145, 2001.
25. S. Thrun. Robotic mapping: A survey. In *Exploring Artificial Intelligence in the New Millennium*. 2002.
26. D. Vlasic et al. Dynamic shape capture using multi-view photometric stereo. *ACM Trans. Graph.*, 28(5), 2009.
27. D. Wagner, T. Langlotz, and D. Schmalstieg. Robust and unobtrusive marker tracking on mobile phones. In *ISMAR*, pages 121–124, 2008.
28. T. Weise, T. Wismer, B. Leibe, and L. V. Gool. In-hand scanning with online loop closure. In *IEEE Int. Workshop on 3-D Digital Imaging and Modeling*, 2009.
29. K. Zhou, M. Gong, X. Huang, and B. Guo. Data-parallel octrees for surface reconstruction. *IEEE Trans. on Visualization and Computer Graphics*, 17, 2011.